Journal of Particle Science and Technology 3 (2017) 219-232

J | P | S | T

http://jpst.irost.ir

Journal of Particle Science and Technology

IROST

Electrophoretic deposition and corrosion behavior study of aluminum coating on AZ91D substrate

Hossein Aghajani*, Maryam Pouzesh

Department of Materials Engineering, University of Tabriz, Tabriz, Iran

HIGHLIGHTS

- In this study, aluminum powder coating was developed on AZ91D magnesium alloy substrate by electrophoretic deposition.
- To determine the optimal condition of deposition, the effects of $AlCl_3.6H_2O$ concentration, applied voltage, and deposition time were investigated.
- A well-stabilized suspension and a uniform deposition were obtained at the $AlCl_3.6H_2O$ concentration of 0.6 mM, applied voltage of 70 V and deposition time of 18 min.

GRAPHICAL ABSTRACT

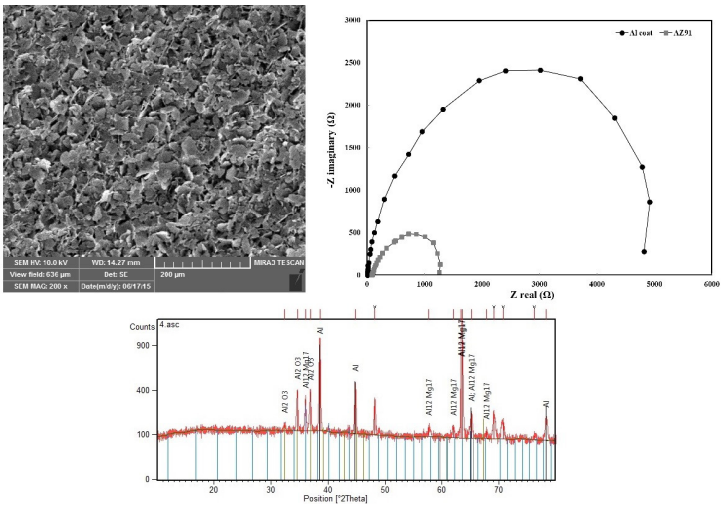

ARTICLE INFO

Article history:

Received 17 December 2017
Revised 10 February 2018
Accepted 12 February 2018

Keywords:

Aluminum coating
Electrophoretic deposition
AZ91D magnesium alloy
Coating morphology
Suspension stability

ABSTRACT

Aluminum coating was prepared on AZ91D magnesium alloy substrate using the electrophoretic deposition (EPD) method in absolute ethanol solvent. In order to determine the optimal concentration of $AlCl_3.6H_2O$ additive, the zeta potential and size of particles in the suspension were measured in the presence of different concentrations of $AlCl_3.6H_2O$. The results showed that an appropriate coating is obtainable in the presence of 0.6 mM $AlCl_3.6H_2O$ as an additive. The effects of applied voltage, deposition time, and additive concentration on deposition weight, deposition thickness, and coating morphology were also studied. A uniform coating with smaller pores and higher density was obtained at the additive concentration of 0.6 mM, deposition time of 18 min, and applied voltage of 70 V. The thickness of this coating was measured at about 256.91 µm. According to the results of corrosion behavior studies, the corrosion current density was measured at 29.16 and 12.85 µA/cm^2 for uncoated and aluminum-coated AZ91D alloy, respectively.

* *Corresponding author: Tel.: +9841-33332472 ; Fax: +9841-33356026 ; E-mail address: h_aghajani@tabrizu.ac.ir*

DOI: 10.22104/JPST.2018.2662.1105

1. Introduction

Magnesium alloys possess excellent mechanical and physical properties such as high specific strength and stiffness, low density [1], high strength-to-weight ratio [2], good electromagnetic shielding [3], great damping capability [4], and satisfactory thermal and electrical conductivity [5,6]. These alloys are widely used in automotive, aerospace, military, electronic [4,7] and ceramic industries [8]. Another application of EPD was reported by [9] to fabricate a YSZ/Al_2O_3 nanostructured composite coating on an iron-nickel based superalloy. Additionally, these alloys suffer from high flammability, low melting point, high chemical activity, and low corrosion resistance, resulting in limited industrial applications [10].

Generally, the corrosion resistance of magnesium alloys can be improved using heat treatment and coating processes [1]. A series of coating methods and surface treatments has been developed to improve the corrosion, wear, and heat resistance of these alloys. Among these methods the electrophoretic deposition (EPD) technique is well-considered with a variety of new applications in coating technology [11-13]. This is not only due to its versatility and ability to combine with various materials, but also because of the simple accessories required for this technique [14,5]. During EPD, charged powder particles dispersed in a liquid medium are moved and deposited on a conductive substrate with the opposite charge by applying a DC electric field [14]. Aluminum has many advantages such as good corrosion resistance, thermal and electrical conductivity, and excellent mechanical properties [15,16].

In the present work, the electrophoretic deposition of aluminum on AZ91D magnesium alloy substrate was studied. The dispersion of the suspensions was investigated in the presence of different concentrations of $AlCl_3 \cdot 6H_2O$. In addition, the effects of applied voltage and deposition time on coating morphology were thoroughly examined. Finally, heat treatment and corrosion studies were performed.

2. Factors affecting EPD

It should be noted that the kinetics of electrophoretic deposition and the deposition quality depend on a large number of parameters which are related to the suspension and its process. The parameters related to the suspension are the particle size, dielectric constant of liquid, conductivity of suspension, viscosity of suspension, zeta potential and stability of suspension. Also, the process related parameters are the concentration of solid in suspension, conductivity of substrate, applied voltage and deposition time.

Some of these parameters are inter-related to one another. It is noted that the quality of electrophoretic deposition depends heavily on the suspension conditions [17]. In general, a stable suspension can provide a better deposition during the EPD process. The stability of suspension can be measured by zeta potential. Generally, its higher absolute value shows a better dispersion of the particles in the suspension. The electrical conductivity of the suspension has an important role in the process during EPD [18]. Experiments have shown that as the ionic concentration in the suspension increases, the conductivity of the suspension increases rapidly [17]. Also, the dielectric constant of the suspending medium directly affects the conductivity of suspension and it increases as the dielectric constant increases [14]. After fixing the suspension parameters, the process parameters can be chosen to have a desired deposition. Normally the amount of deposit increases as the applied voltage increases. Similarly, a higher deposition rate is expected with increasing particle concentration and deposition time [14].

3. Experimental procedure

Aluminum powder (Sigma-Aldrich, 99.5%) with a flake shape and a mean particle size of <5 μm was used as the raw material. Aluminum chloride hexahydrate $AlCl_3 \cdot 6H_2O$ (Beijing Guohua Chemical Factory, China) was employed as the additive, and absolute ethanol (99.6%) was used as the solvent. The Al powder (10 g/l) was dispersed in ethanol and different amounts of $AlCl_3 \cdot 6H_2O$ (0.1-5 mM) were added to the suspensions. The suspensions were magnetically stirred for 24 hours and then ultrasonically deflocculated for 180 min to prepare a well-dispersed stable suspension.

An AZ91D magnesium alloy with a thickness of 2 mm and working area of 1.44 cm^2 was utilized as the substrate (cathode). In addition, a low-carbon 316 stainless steel with the same working area and a thickness of 0.1 mm was used as the anode. The distance between the two parallel electrodes was fixed at 1.2 cm during deposition.

The EPD of Al particles was performed using additive concentrations in the range of 0.1 to 5 mM, applied voltage in the range of 10 to 80 V, and deposition time in the range of 2 to 18 min. The zeta potential of the suspensions with different concentrations of $AlCl_3 \cdot 6H_2O$ was measured using a zeta potential analyzer (Malvern-HSA3000), and the deposit weight was measured by weighing the cathode before and after deposition (RADWAG ± 0.0001 g). The surface morphology and thickness of coatings were studied by scanning electron microscopy (FE-SEM, TESCAN-MIRA3 FEG). The size of particles in the suspensions was determined using the dynamic light scattering (DLS) system (Microtrac Nanotrac Wave). Finally, the corrosion behavior of the coating was examined using the electrochemical impedance spectrum.

4. Results and discussion

The kinetics of electrophoretic deposition and coating quality is highly dependent on a number of parameters, e.g. applied voltage, additive concentration, deposition rate, and substrate conductivity. Hence, a proper control mechanism should be considered on individual parameters in the process of electrophoretic deposition [14,19].

4.1. Effect of $AlCl_3 \cdot 6H_2O$ concentration on zeta potential

Yang et al. studied the influence of $AlCl_3 \cdot 6H_2O$ additive concentration on the stability of aluminum suspensions and rate of deposition were studied [20]. The results showed that positively charged particles of aluminum should be deposited on the cathodic substrate during the deposition process. While the deposition rate is directly related to zeta potential, zeta potential is much lower in the alkaline range than the acidic range [14]. Zeta potential increases and acidity decreases with an increase in additive concentration [21]. Zeta potential has more impact on the stability of the suspension and electrophoretic mobility and can be changed by adding additives such as $AlCl_3 \cdot 6H_2O$. The effect of additive concentration on the zeta potential of ethanol-contained suspension of aluminum particles is depicted in Figure 1.

It should be noted that the amount and type of additive has a great influence on the charging of the particles present in the suspension. All zeta potentials are positive including the suspension without $AlCl_3 \cdot 6H_2O$. This indicates that positively charged Al particles should be deposited on the cathode substrate. For a suspension without $AlCl_3 \cdot 6H_2O$, a reasonable mechanism to adjust the charge is to produce H^+ ions from small amounts of existing H_2O in the commercial alcohol by electrolytic dissociation, and then absorb these onto the aluminum particles to make them electrified. When metal ions are introduced into the suspension through the addition of $AlCl_3 \cdot 6H_2O$, the resulting aluminum alkoxide and aluminum hydroxide ions are absorbed on the surface of aluminum particles and make a surface charge density [20].

Based on Figure 1, zeta potential increases as the $AlCl_3 \cdot 6H_2O$ concentration is increased up to 1 mM, but then decreases with further increases in the additive concentration. It can be concluded that the increase in zeta potential is due to the enhancement of metal ions in the suspension as a result of additive concentration enhancement. Thus, the density of particle surface charge increases with the absorption of aluminum hydroxide and aluminum alkoxide on the aluminum particles in the suspension. In addition, by increasing the surface charge the electrostatic repulsion force increases between the particles leading to zeta potential enhancement.

Increasing the metal ions and their attraction on the surface of aluminum particles may reduce the thickness of the electrical double layer. This may lead to a reduction in repulsive forces between particles; and consequently, a reduction in zeta potential. Therefore, the reduction of zeta potential in 1.5 mM additive concentration can be attributed to the reduced thickness of the electrical double layer. Nevertheless, higher zeta potential values may be undesirable during the deposition process since they may lead to an excessively conductive suspension and a reduction of electrophoretic mobility.

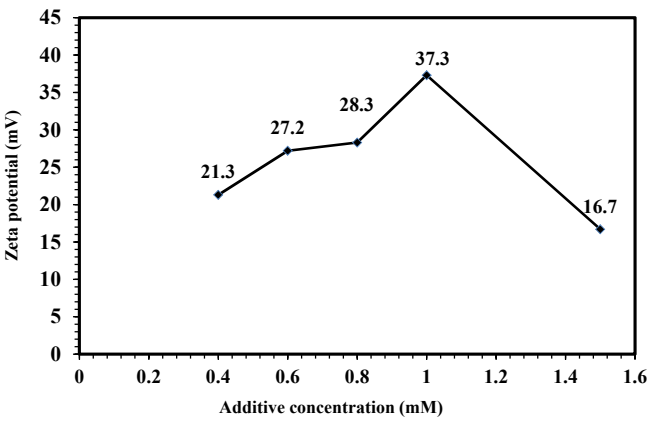

Fig. 1. Zeta potential as a function of additive concentration for Al particles in ethanol.

4.2. Effect of $AlCl_3 \cdot 6H_2O$ concentration on the size of particles

The effect of additive concentration on the size of particles is demonstrated in Figure 2. Although there is no general rule for determining the size of particles for electrophoretic deposition, a suitable deposition has been reported in the range of 1 to 20 µm [14]. According to Figure 2, the size of particles in suspensions in the presence of 0.4 to 1.5 mM additive is in the range of 1 to 5 µm. At low additive concentrations, there are few free ions such as aluminum hydroxide and aluminum in the suspension, proving little surface charge on the particles. Therefore, the electrostatic repulsion force necessary for separating the particles is not provided, which can lead to particle agglomeration and increased size.

By increasing the additive concentration up to 0.6 mM, the amount of free ions increased, leading to the enhancement of surface charge on the surface of aluminum particles. Then, the electrostatic repulsion force between particles increased and prevented particle agglomeration. By further increasing the additive concentration up to 1.5 mM, the amount of metal ions and conductivity of the suspension increased. However, the excessive amount of metal ions causes a reduction in the thickness of the electrical double layer. In this case, the particles agglomerate and the size of particles increases. Results revealed that the suspension with the additive concentration of 0.6 mM was a well-stabilized suspension because it had fine particles and an acceptable zeta potential value.

4.3. Effect of applied voltage on deposition rate and coating morphology

The surface morphologies of aluminum coatings in the presence of 0.6 mM $AlCl_3 \cdot 6H_2O$ at various applied voltages are illustrated in Figure 3. In this figure, white areas indicate coated aluminum particles and gray and black areas represent the porosities or less-coated surface of the substrate. A comparison between the results shows that the coating deposited at the applied voltage of 70 V (Figure 3e) is denser than the others.

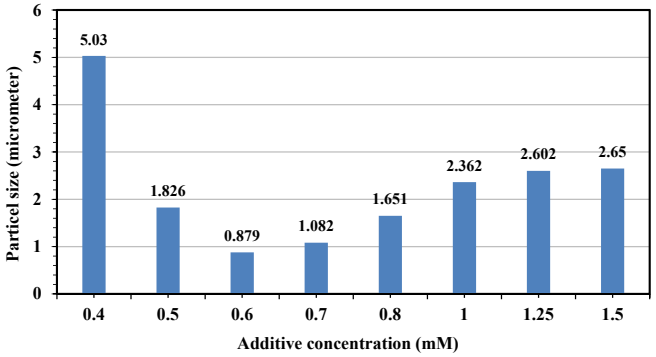

Fig. 2. Size of particles as a function of additive concentration for .Al particles in ethanol

The surface morphology of the coatings in the presence of 1 mM $AlCl_3 \cdot 6H_2O$ and different applied voltages are demonstrated in Figure 4. It is clear that the coating deposited at the applied voltage of 30 V has a lower porosity. By further increasing the applied voltage up to 40 V, the porosities increase and a non-uniform coating forms due to the high velocity of particles.

The deposition weight as a function of applied voltage for the deposition time of 3 min is depicted in Figure 5. According to this figure, by increasing the applied voltage up to 70 V, the deposition weight increases and then decreases for both 0.6 mM and 1mM additive concentrations. At applied voltages higher than 70 V turbulent currents are created which may damage the coating and affect its quality, leading to a reduction in deposition weight.

Figure 5 shows that in the case of 1mM additive concentration the weight of deposition increases slowly at applied voltages lower than 50 V and causes the creation of a uniform coating. However at applied voltages higher than 50 V, the rate of deposition is high leading to the agglomeration of particles and creation of a non-uniform deposition. Therefore, in the presence of 1 mM additive concentration, an applied voltage of lower than 50 V is required to deposit a uniform coating. According to Figures 3 and 5, the applied voltage of 30 V was chosen as the appropriate voltage to have a deposition with a lower porosity and higher homogeneity. In addition, in the case of 0.6 mM additive concentration, voltage of 70 V was selected as the optimum value due to the dense structure and high coating weight shown in Figures 4 and 5, respectively.

4.4. Effect of $AlCl_3 \cdot 6H_2O$ concentration on coating morphology

The surface morphology of coatings for 0.6 and 1 mM additive concentrations are illustrated in Figure 6. Additive concentration affects the viscosity of the suspension. The relationship between viscosity and zeta potential is presented in Eq. (1), which shows that

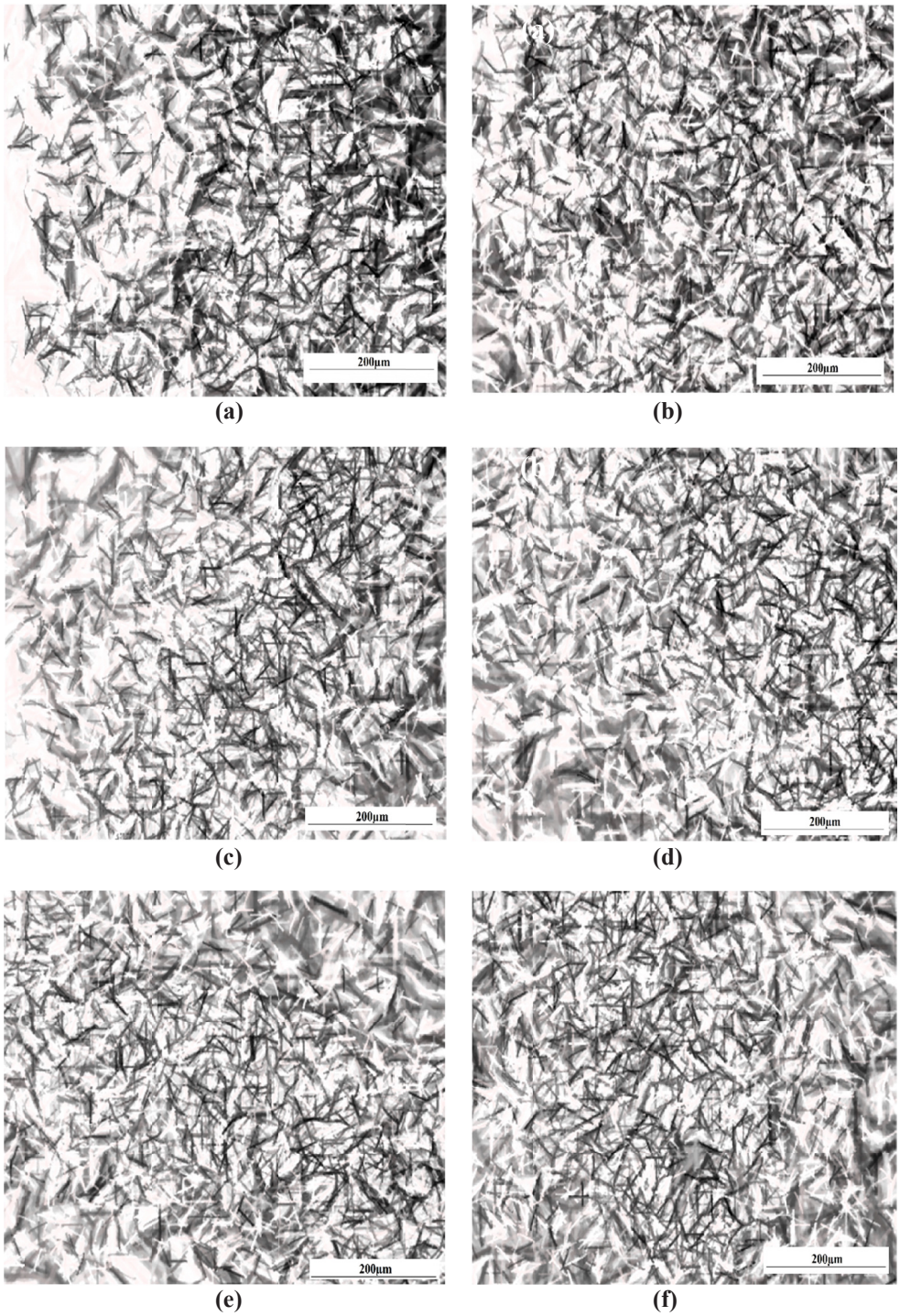

Fig. 3. Optical microscope images of aluminum coatings at different applied voltages for 0.6 mM additive concentration and 5 min deposition time, (a) 30 V, (b) 40 V, (c) 50 V, (d) 60 V, (e) 70 and (f) 80 V.

that appropriate conditions for homogeneous deposition can be provided with maximum zeta potential and minimum viscosity [14].

$$\mu = \frac{\varepsilon \varepsilon_0 \xi}{\eta} \quad (1)$$

where ξ, η, ε_0, ε and μ denote the zeta potential of particles, viscosity of the solvent, vacuum permittivity coefficient, relative permittivity coefficient of the solvent, and electrophoretic mobility, respectively.

As mentioned before, the zeta potential and surface charge of particles increase by increasing additive concentration. In addition, the number of metal ions in the suspension increases. In this case, the majority of the current is carried by free ions in the suspension and only a small portion of it is assigned for the movement of charged particles. Thus, it results in the agglomeration of particles and reduction of electrophoretic mobility.

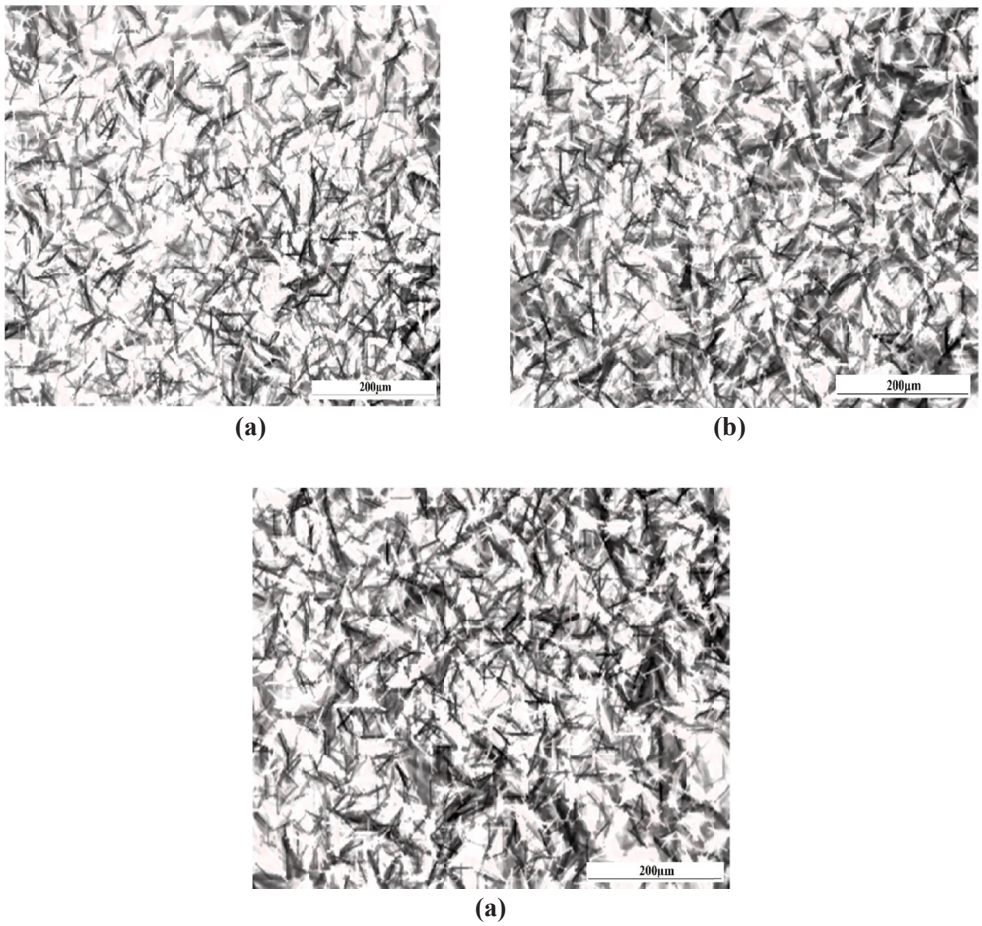

Fig. 4. Optical microscope images of aluminum coatings for 5 min deposition time and 1 mM additive concentration. (a) 30 V, (b) 35 V, and (c) 40 V.

charged particles. Thus, it results in the agglomeration of particles and reduction of electrophoretic mobility.

Figure 6 indicates that uniform deposits can be achieved in the presence of 0.6 mM additive concentration. Moreover, the agglomeration of particles in this suspension; and subsequently, the pores in the coating microstructure are less than those of the 1 mM suspension. As a result, the surface morphology of the coating deposited from the 1 mM suspension is coarse and large porosities are observable in this coating.

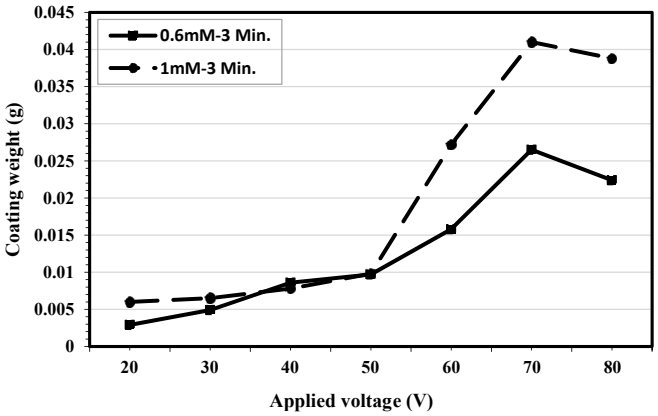

Fig. 5. The coating weight as a function of the applied voltage at 3 min deposition time.

4.5. Effect of deposition time on deposition rate and coating morphology

In order to evaluate the effect of deposition time on deposition weight and its morphology, the structures of coatings deposited at a constant voltage are compared. The surface morphology of aluminum coatings at different deposition times and constant applied voltage of 70 V for 0.6 mM additive concentration is presented in Figure 7. At the initial times of deposition the concentration of particles in the suspension was high, but the time was not adequate for deposition of particles on the surface of the substrate. Therefore, the surface is not completely covered by Al particles and the coatings are not uniform and have a low density.

According to Figure 7, it is clear that a uniform deposition with minimum porosity and high density is obtainable at the deposition time of 18 min. By further increasing the deposition time up to 20 min, the

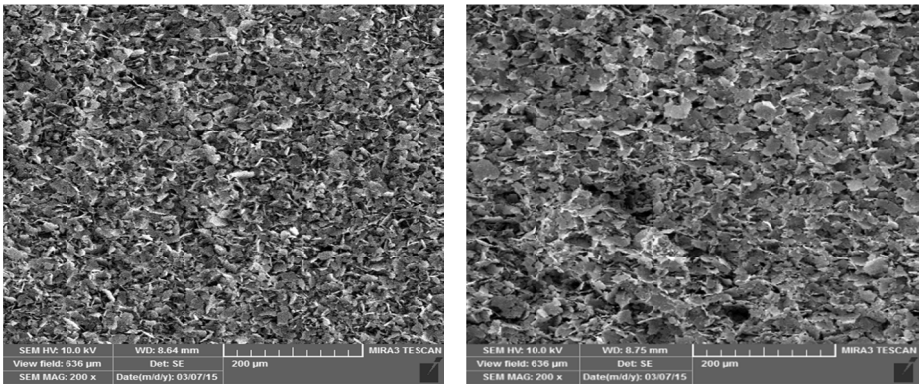

(a) **(b)**

Fig. 6. The surface morphology of aluminum coatings for (a) 0.6 mM and (b) 1 mM concentrations of $AlCl_3.6H_2O$ (deposition time: 18 min, applied voltage for 0.6 and 1 mM: 70V and 30V, respectively).

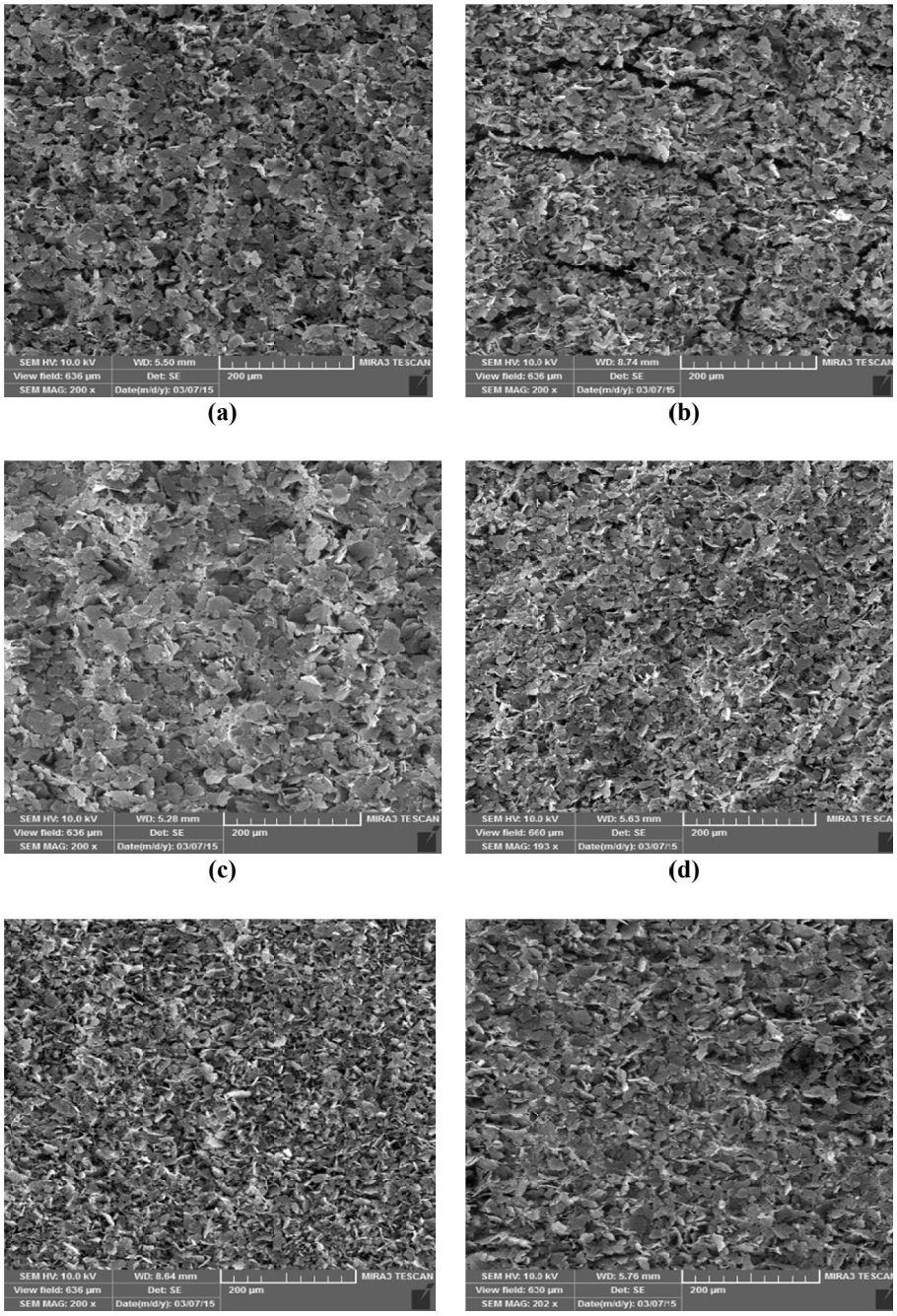

(c) **(d)**

(e) **(f)**

Fig. 7. SEM images of surface of the coatings for 0.6 mM additive concentration, coated for (a) 2, (b) 6, (c) 10, (d) 12, (e) 18, and (f) 20 min.

concentration of particles in the suspension decreased and the electrical resistance of the substrate increased. This phenomenon causes the detachment of particles from the coating and reduction of the deposition weight.

The surface morphology of aluminum coatings at the constant applied voltage of 30 V, additive concentration of 1 mM, and various deposition times is shown in Figure 8. It is clear that at the initial times of deposition the substrate surface is not completely covered with coating and contains a low-density layer. Although the density of the coating increases by increasing the deposition time, several large pores are seen in the coating structure (Figure 8d) due to the high concentration of metal ions, this leads to a reduction in the electrophoretic mobility and enhancement in viscosity.

The variation of coating weight versus the deposition time is depicted in Figure 9 for two different additive concentration values. It is obvious that at initial deposition times the weight of deposition increases with time and reaches the highest value in 18 min. By further increasing the deposition time up to 20 min, the deposition weight decreases in both concentrations

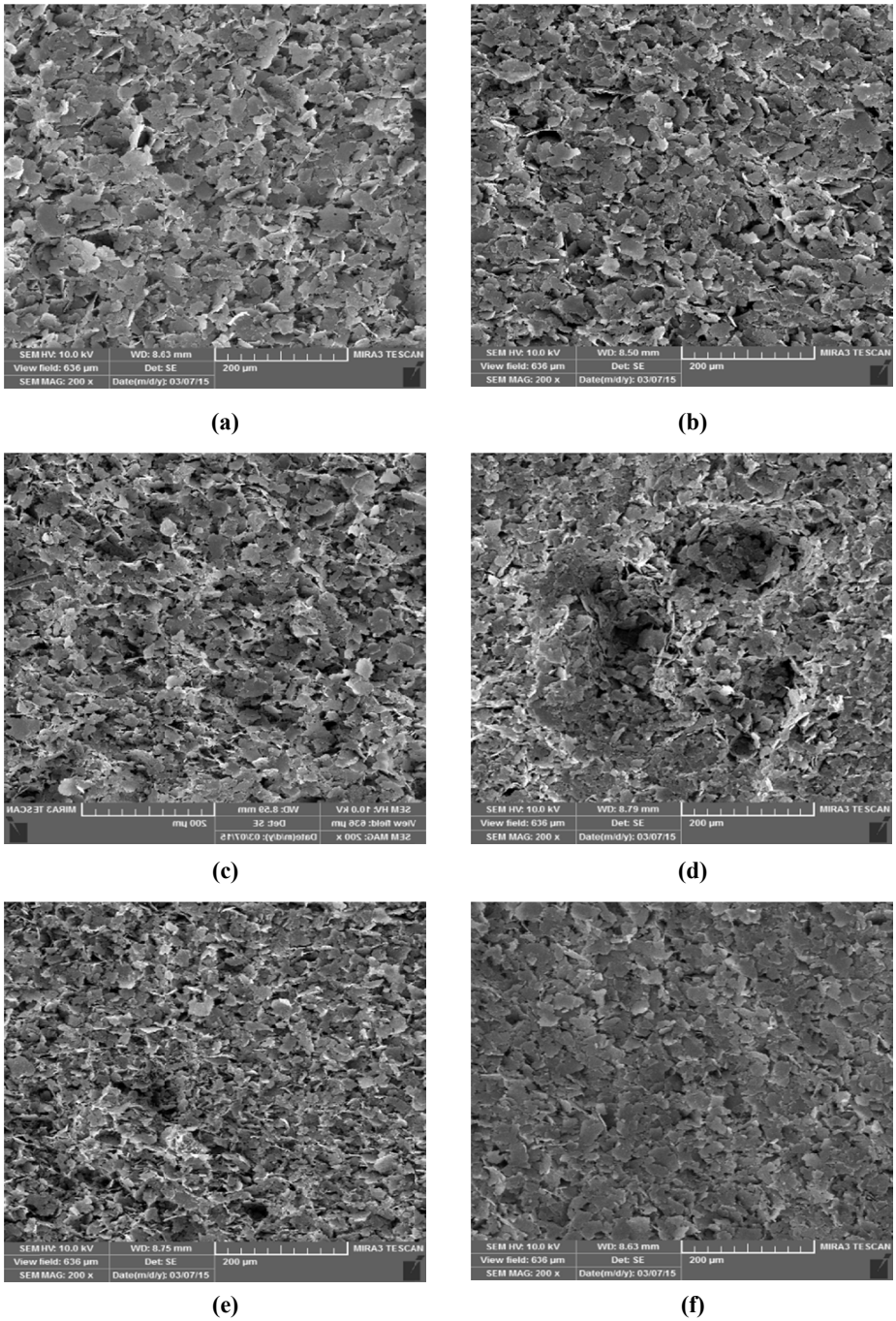

Fig. 8. SEM images of surface of the coating for 1 mM additive concentration, coated for (a) 2, (b) 6, (c) 10, (d) 12, (e) 18 and (f) 20 min.

due to the reduction of suspension concentration and enhancement of the electrical resistance of the substrate. From Figure 9, it is clear that the coating weight for 0.6 mM additive concentration is greater than that of the 1 mM one. This behavior is because of the higher stability of the suspension with 0.6 mM additive concentration. As a result, the particles retain their stability even during prolonged times of deposition leading to less settlement and enhancement of deposition weight.

4.6. Thickness analysis of depositions

Scanning electron microscopy (SEM) was used in order to determine the thickness of coatings. The cross-section images of the coatings for both 0.6 and 1mM additive concentrations at two different deposition times are demonstrated in Figure 10. Coating thickness increased as the deposition time increased. The comparison between the cross-sectional views of the coatings show that the thickness of deposition at 1 mM additive concentration is greater than the 0.6 mM one, while the obtained coating weight is higher in 0.6 mM than 1 mM. This is due to the formation of a dense and uniform coating during deposition in the presence of 0.6 mM additive concentration.

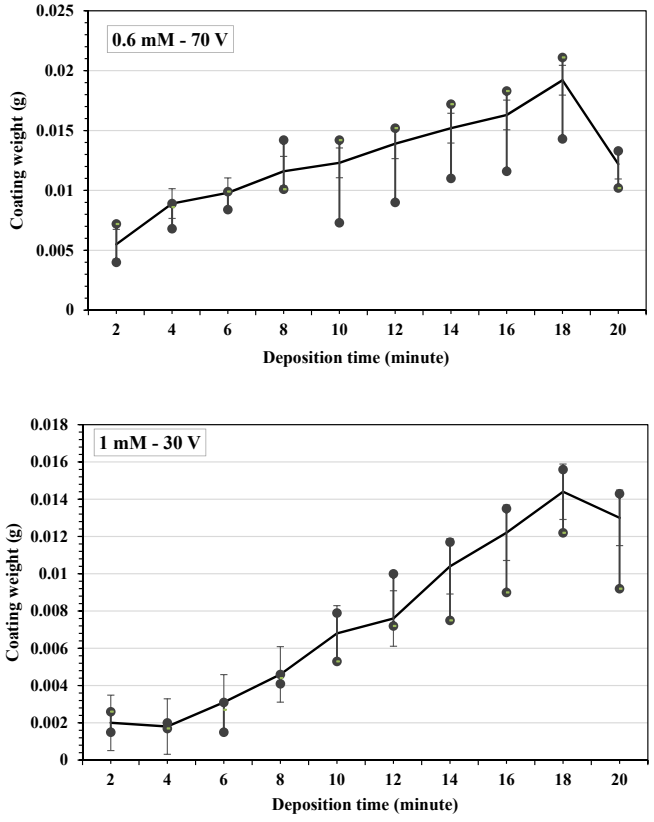

Fig. 9. Coating weight versus deposition time.

According to the obtained results, the coating with the additive concentration of 0.6 mM, deposition time of 18 min, and applied voltage of 70 V, is a suitable coating and has appropriate thickness (256.91 μm), weight (0.019 g), and density of deposition.

4.7. Heat treatment and microstructural studies

In order to improve the adhesion and density of the green coating, the heat treatment of the optimum coating was carried out at 400 °C for 1 hour. After heat treatment, in order to decrease the probability of crack formation, the sample was slowly cooled in the furnace chamber. To determine the density and adhesion of the coating to substrate, the surface morphology was studied using SEM analysis and the results are provided in Figure 11.

It is clear that heat treatment reduced the porosities and increased the density of the coating. This may be due to the expansion of aluminum particles, their oxidization with increasing temperature, and the formation of an alumina phase. On the other hand, the coating has a high adhesion strength due to the formation of an intermetallic β phase ($Mg_{17}Al_{12}$) at the interface of substrate and coating.

In order to determine the resulted phases in the obtained coating, X-ray diffraction analysis (XRD) and energy dispersive spectroscopy (EDS) were utilized. The results of XRD analysis after heat treatment are shown in Figure 12. The results indicated that, beside the metallic FCC aluminum phase, Al_2O_3 and $Mg_{17}Al_{12}$ phases are detected in the coating structure. The Al_2O_3 phase is formed due to the reaction of aluminum with oxygen in the air, and the intermetallic phase of β ($Mg_{17}Al_{12}$) is formed due to the melting of the substrate surface during the heat treatment, which can improve the coating adhesion to the substrate.

Al and Al_2O_3 peaks gradually increase and the peaks of $Mg_{17}Al_{12}$ decrease as the coating thickness increases. The alumina (Al_2O_3) phase formed during heat treatment plays the role of sintering aid and compensates for the volume shrinkage caused by sintering. This phenomenon leads to the enhancement of the density and adhesion of the coating. The formation of a β ($Mg_{17}Al_{12}$) phase at the interface of the coating and substrate improves the adhesion of the coating to the substrate.

The results of EDS analysis of the samples before and after heat treatment are presented in Figure 13. The amounts of elements present in the coatings before and

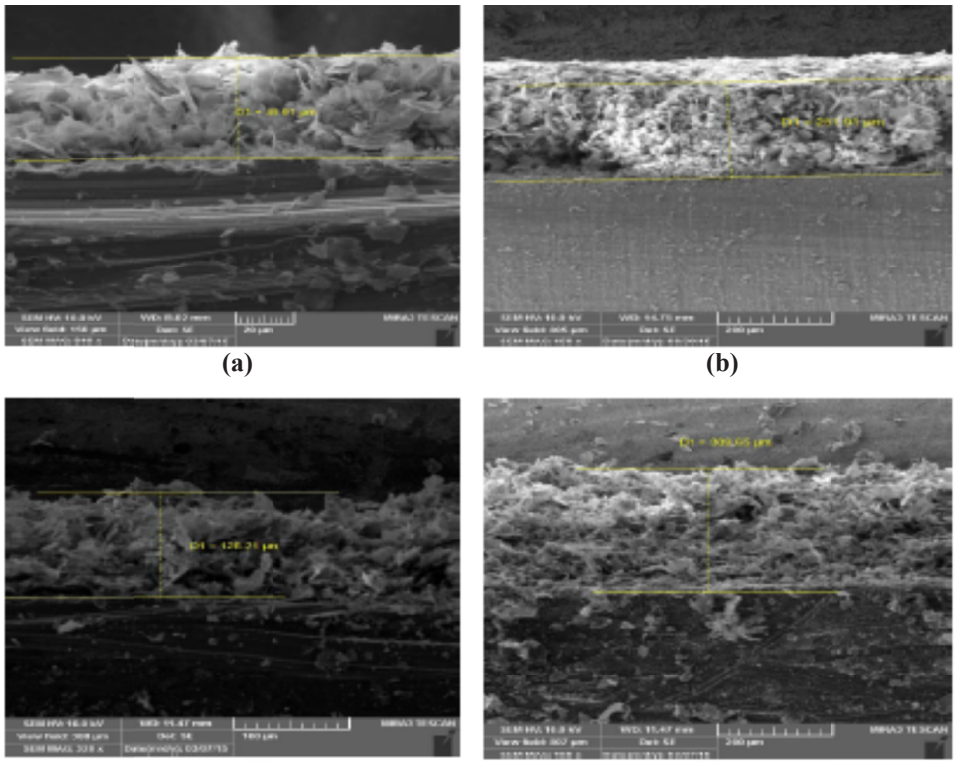

Fig. 10. SEM images of the cross-section of coated samples (a) 2 min, 70 V, 0.6 mM; (b) 18 min, 70 V, 0.6 mM; (c) 2 min, 30 V, 1 mM and (d) 20 min, 30 V, 1 mM.

after heat treatment are given in Figure 14. It is obvious that the weight percentage of Mg and O elements increased and the weight percentage of Al decreased after heat treatment.

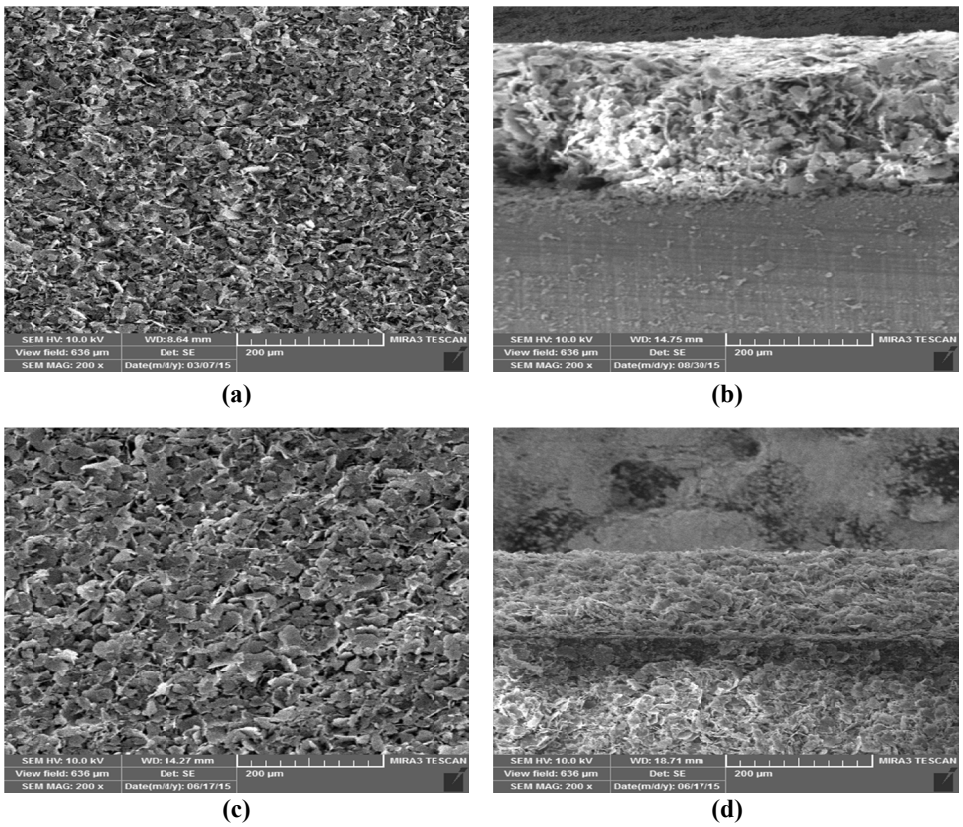

Fig. 11. SEM images of surface and cross-section of the coatings, (a) surface and (b) cross-section of the sample before heat treatment, (c) surface and (d) cross-section of the sample after heat treatment at 400 ° C for 1 hour.

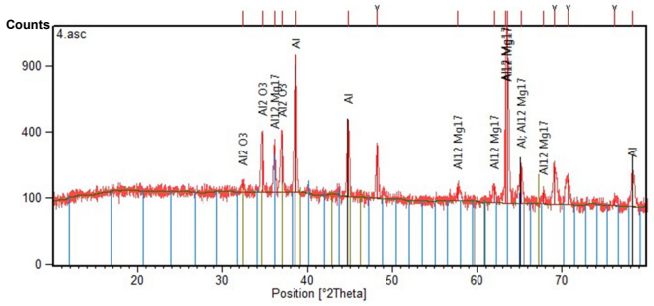

Fig. 12. Results of XRD analysis after heat treatment.

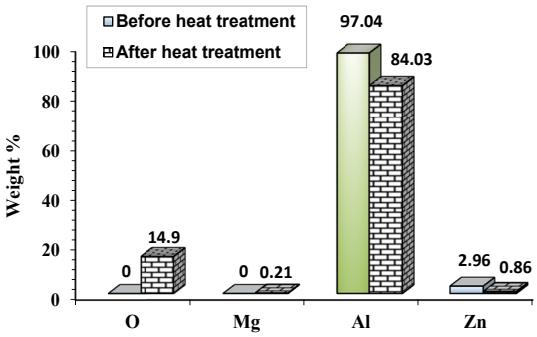

Fig. 14. Percentage of element weights before and after heat treatment.

4.8. Corrosion resistance analysis

The corrosion resistance study of the uncoated and aluminum-coated AZ91D magnesium alloy was performed by polarization and impedance tests. To this end, a solution of 3.5% NaCl was used. Figure 15 illustrates the potentiodynamic polarization curves of both samples.

Polarization resistance, which shows the resistance to transmission time, is calculated using the polarization test results as follows [22]:

$$R_p = \frac{\beta_a \times \beta_c}{2.303 \times i_{corr} \times (\beta_a + \beta_c)} \quad (2)$$

where β_a and β_c are slopes of the Tafel anode and cathode (V/decade), respectively. The i_{corr} denotes the corrosion current (amperes). Also, the corrosion rate (CR) in terms of milligrams per year (mpy) can be calculated as [22]:

$$mpy = \frac{K \times M \times i_{corr}}{Z \times D \times F} \quad (3)$$

in which M is the base metal atomic mass (in g), D shows the density in g/cm^3, F represents the Faraday constant, Z refers to the atomicity, and K=0.129. Table 1 shows the parameters of dynamic polarization test for uncoated and coated samples.

Corrosion current density is associated with the resistance to corrosion. Based on Figure 15, the corrosion current density for the coated sample is less than that of the AZ91D alloy, reflecting the higher corrosion resistance of the coated sample compared to the uncoated one. Moreover, both coated and uncoated samples have an active behavior in the 3.5% NaCl solution and the passive area was not found.

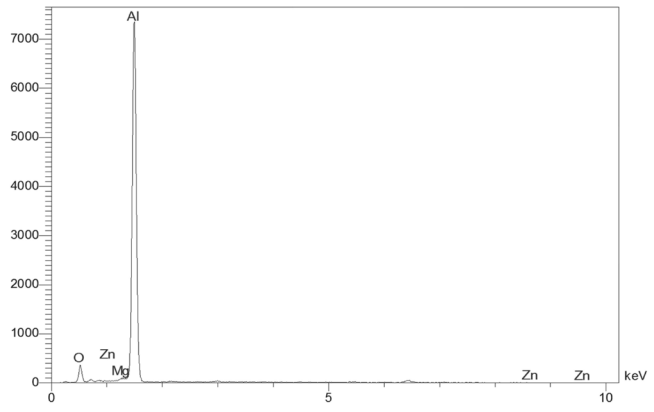

Element	Line	Intensity	Weight %	Atomic %
O	Ka	0.0	0.00	0.00
Mg	Ka	0.0	0.00	0.00
Al	Ka	4423.5	97.04	98.75
Zn	Ka	8.2	2.96	1.25
			100.00	100.00

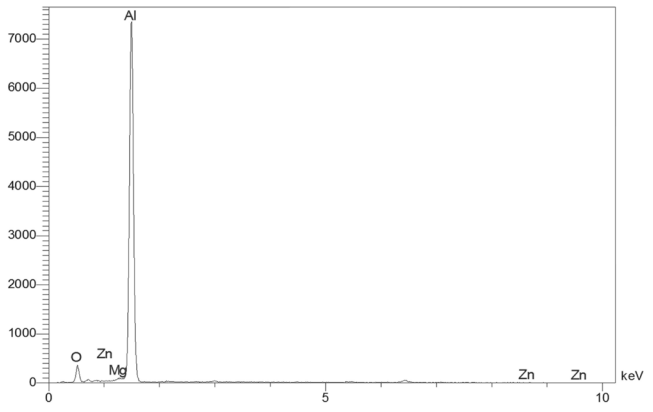

Element	Line	Intensity	Weight %	Atomic %
O	Ka	206.3	14.90	22.90
Mg	Ka	15.6	0.21	0.21
Al	Ka	6170.8	84.03	76.56
Zn	Ka	3.9	0.86	0.32
			100.00	100.00

Fig. 13. EDS analysis of cross-section (a) before heat treatment and (b) after heat treatment.

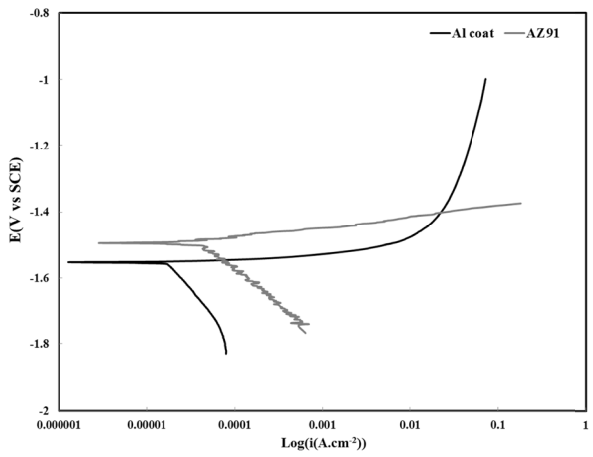

Fig. 15. Polarization curve of uncoated and aluminum coated AZ91D magnesium in salt solution NaCl 3.5%.

According to Table 1, the coated sample has a lower corrosion and higher corrosion resistance in comparison with the uncoated AZ91D magnesium, which is due to the higher cathodic potential of aluminum in comparison with AZ91D magnesium alloy. This fact leads to the protection of the substrate from corrosive solution in the presence of aluminum coating.

The presence of cracks and open porosities in the coating can provide a path for the corrosive solution to reach to the substrate, which subsequently leads to galvanic corrosion between the cathodic aluminum coating and anode magnesium substrate. Hence, the thickness and density of the coating must be modified in such a way to minimize galvanic corrosion. The passive layer of alumina and aluminum hydroxide can be a barrier against the penetration of corrosive solution, and corrosion resistance can be improved. The Nyquist curves of uncoated and aluminum-coated AZ91D samples in the 3.5 wt% NaCl solution are shown in Figure 16. The capacitive ring diameter in the Nyquist curve represents the polarization resistance (resistance to corrosion) of the electrode. A higher polarization resistance represents a lower corrosion rate. According to Figure 16, the capacitive ring for the coated AZ91D alloy is much bigger than that of the uncoated one, showing that the corrosion rate of the coated sample is lower than that of the uncoated sample. The results obtained from the electrochemical impedance test confirmed the results obtained from the polarization test. Both methods emphasized enhancing the corrosion resistance of AZ91D alloy in the presence of aluminum coating.

The results of electrochemical impedance spectroscopy can be simulated using an appropriate electrical equivalent circuit such as the one illustrated in Figure 17 [23]. The equivalent impedance analysis describes the behavior of the corrosion resistance of the coating. In Figure 17, R_s denotes the uncompensated solution resistance, R_{ct} indicates the charge transfer resistance or corrosion resistance on the metal interface and dual layer, Rcoat shows the coating resistance, CPE_{dl} represents the electric double layer capacitor, and the CPE_{coat} refers to the capacitor of coating.

The equivalent impedance of the circuits in Figure 17 can be written as the following, respectively:

$$Z_t = Z(R_s) + Z(R_{ct} \parallel CPE_{dl}) = R_s + \frac{R_{ct}}{R_{ct}\, jCPE_{dl}\omega + 1} = Z' + j\,Z'' \quad (4)$$

$$Z_t = Z(R_s) + \frac{(Z(R_{ct} \parallel CPE_{dl}) + Z(R_{coat})) \times Z_{CPE_{coat}}}{(Z(R_{ct} \parallel CPE_{dl}) + Z(R_{coat})) + Z_{CPE_{coat}}} \quad (5)$$

$$Z_t = R_s + \frac{R_{coat} + R_{ct} - R_{coat}\, R_{ct}\, CPE_{coat}\, CPE_{dl}\, \omega^2}{(1 - R_{coat}\, R_{ct}\, CPE_{coat}\, CPE_{dl}\, \omega^2) + j(R_{coat}(CPE_{coat} + CPE_{dl}) + R_{ct}\, CPE_{coat})\omega}$$

The parameters of equivalent circuit in Figure 17 are provided in Table 2.

Table 1. Results of dynamic polarization test in 3.5 wt% NaCl solution.

Samples	Corrosion current density ($\mu A.cm^{-2}$)	Corrosion potential (mV vs SCE)	β_a (mV/decade)	β_c (mV/decade)	R_p (Ω)	C.R. (mpy)
AZ91D	29.16	-1490.96	39.48	229.79	501.69	26.3
Aluminum coated AZ91D	12.85	-1553.5	43.46	203.33	1209.95	11.59

Table 2. Equivalent circuit parameters.

Samples	R_S ($\Omega.cm^2$)	$CPET_{dl}$ ($\mu F.cm^{-2}$)	$CPEP_{dl}$	R_{ct} ($\Omega.cm^2$)	$CPET_{coat}$ ($\mu F.cm^{-2}$)	$CPEP_{coat}$	Rcoat ($\Omega.cm^2$)
Uncoated AZ91D	12.1	13.9	0.8	1615.7	---	---	---
Aluminum coated AZ91D	14.2	6.75	0.9	1729.2	2.7	0.9	5637.6

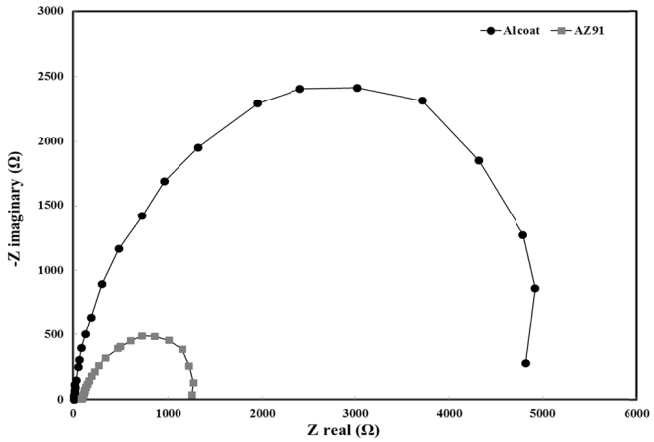

Fig. 16. AC electrochemical impedance spectrum of coated and uncoated AZ91D sample in the solution of NaCl 3.5 wt%.

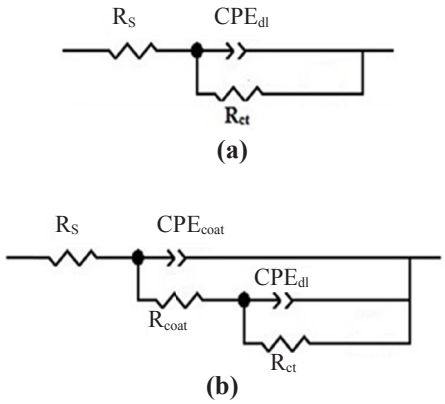

Fig. 17. The equivalent circuit for the impedance spectrum analysis, (a) uncoated AZ91D alloy and (b) AZ91D alloy coated with aluminum [23].

5. Conclusion

In this paper, aluminum coating was developed on an AZ91D magnesium alloy substrate by electrophoretic deposition. To determine the optimal condition of deposition the effect of $AlCl_3.6H_2O$ concentration, applied voltage, and deposition time was investigated. The DLS analysis showed that the size of the particles in the suspension varies from 1 to 5 μm for the additive concentration in the range of 0.4 to 1.5 mM. A well-stabilized suspension and a uniform deposition were obtained at the $AlCl_3.6H_2O$ concentration of 0.6 mM. The zeta potential value and mean size of particles for this suspension were measured at 27.2 mV and 0.879 μm, respectively. Surface morphology studies showed that a uniform and low-pore coating from this suspension is obtainable at the applied voltage of 70 V and deposition time of 18 min.

References

[1] F. Czerwinski, Magnesium Alloys: Corrosion and Surface Treatments, InTech Publisher, London, 2011, pp. 195.

[2] G.L. Song, "Electroless" deposition of a pre-film of electrophoresis coating and its corrosion resistance on a Mg alloy, Electrochim. Acta, 55 (2010) 2258-2268.

[3] W. Feng, W. Yue, M.Ping-li, Y.U. Bao-yi, G. Quan-ying, Effects of combined addition of Y and Ca on microstructure and mechanical properties of die casting AZ91 alloy, T. Nonferr. Metal. Soc. 20 (2010) s311-s317.

[4] Y. Zhan, Z. Hong-yang, H. Xiao-dong, J. Dong-ying, Effect of elements Zn, Sn and In on microstructures and performances of AZ91 alloy, T. Nonferr. Metal. Soc. 20 (2010) s318-s323.

[5] A. Nold, J. Zeiner, T. Assion, R. Clasen, Electrophoretic deposition as rapid prototyping method, J. Eur. Ceram. Soc. 30 (2010) 1163-1170.

[6] Y. Tao, T. Xiong, C. Sun, L. Kong, X. Cui, T. Li, G.L. Song, Microstructure and corrosion performance of a cold sprayed aluminum coating on AZ91D magnesium alloy, Corros. Sci. 52 (2010) 3191-3197.

[7] S. Fleming, An Overview of magnesium based alloys for aerospace and automotive applications, [Dissertation] Rensselaer Polytechnic Institute, Hartford, CT August, 2012.

[8] A. Shahriari, H. Aghajani, Electrophoretic deposition of 3YSZ coating on AZ91D using an aluminum interlayer, Prot. Met. Phys. Chem. S. 53 (2017) 518-526.

[9] M. Ahmadi, H. Aghajani, Structural characterization of YSZ/Al_2O_3 nanostructured composite coating fabricated by electrophoretic deposition and reaction bonding, Ceram. Int. 44 (2018) 5988-5995.

[10] S. Candan, M. Unalb, E. Koc, Y. Turen, E. Candan. Effects of titanium addition on mechanical and corrosion behaviours of AZ91 magnesium alloy, J. Alloy. Compd. 509 (2011) 1958-1963.

[11] K. Yang, Z. Jiang, J. Chung, Electrophoretically Al-coated wire mesh and its application for catalytic oxidation of 1,2-dichlorobenzene, Surf. Coat. Tech. 168 (2003) 103-110.

[12] G. Lee, S. Pyun, C. Rhee, A study on electrophoretic deposition of Ni nanoparticles on pitted Ni alloy 600 with surface fractality, J. Colloid Interf. Sci. 308

(2007) 413-420.

[13] X. Guo, X. Li, H. Li, D. Zhang, C. Lai, W. Li, A Comprehensive investigation on the electrophoretic deposition (EPD) of Nano-Al/Ni energetic composite coatings for the combustion application, Surf. Coat. Tech. 265 (2015) 83-91.

[14] L. Besra, M. Liu, A review on fundamentals and applications of electrophoretic deposition (EPD), Prog. Mater. Sci. 52 (2007) 1-61.

[15] K. Liu, Q. Liu, Q. Han, G. Tu, Electrodeposition of Al on AZ31 magnesium alloy in TMPAC-$AlCl_3$ ionic liquids, T. Nonferr. Met. Soc. 21 (2011) 2104-2110.

[16] ASM International Handbook Committee, ASM Handbook of properties and selection: Nonferrous alloys and special-purpose materials, Vol. 2, ASM International, Ohio, 1990.

[17] J. Ma, W. Chen, Deposition and packing study of sub-micron PZT ceramics using electrophoretic deposition, Mater. Lett. 56 (2002) 721-727.

[18] N. Sato, M. Kawachi, K. Noto, N. Yoshimoto, M. Yoshizawa, Effect of particle size reduction on crack formation in electrophoretically deposited YBCO films, Physica C, 357-360 (2001) 1019-1022.

[19] Z. Wang, J. Shemilt, P. Xiao, Fabrication of ceramic composite coatings using electrophoretic deposition, reaction bonding and low temperature sintering, J. Eur. Ceram. Soc. 22 (2002) 183-189.

[20] L. Yang, X. Wu, D. Weng, Development of uniform and porous Al coatings on FeCrAl substrate by electrophoretic deposition, Colloid. Surface. A, 287 (2006) 16-23.

[21] S. Kim, S. Cho, J. Lee, S. Samal, H. Kim, Relationship between the process parameters and the saturation point in electrophoretic deposition, Ceram. Int. 38 (2012) 4617-4622.

[22] M.G. Fontana, Corrosion engineering, Third Edition, McGraw Hill, New York, 1987.

[23] A. Lasia, Electrochemical impedance spectroscopy and its applications, Springer-Verlag, New York, 2014.